

Synthesis of Cu(OH)₂ Nanowires at Aqueous–Organic Interfaces

Xinyu Song, Sixiu Sun,* Weimin Zhang, Haiyun Yu, and Weiliu Fan

Department of Chemistry, Shandong University, Jinan, 250100, People's Republic of China

Received: August 3, 2003; In Final Form: February 2, 2004

Cu(OH)₂ nanowires have been successfully synthesized at the organic–aqueous interface by the interaction of the copper–bis(2-ethylhexyl) phosphate complex in the organic layer with NaOH in aqueous layer. The nanowires have an average length of 4 μm and are several nanometers in width. CuO nanowires and short whiskers are conveniently prepared through dehydration of Cu(OH)₂ at high concentrations of NaOH under ambient conditions. Transmission electron microscopy and X-ray diffraction techniques have been used to characterize the microstructures and morphologies of the nanowire materials.

Introduction

One-dimensional (1D) materials, especially nanorods and nanowires, have been the focus of considerable interest because of their fundamental importance and potential applications in constructing nanoscale electronic and optoelectronic devices.^{1,2} Many methods have already been developed for the fabrication of 1D materials, including the vapor-phase transport^{3,4} laser-ablation,^{5,6} chemical vapor deposition,⁷ arc-discharge,⁸ template-based,⁹ and solution-chemistry methods.^{10–13} Among these methods, the solution-chemistry methods have potential advantages of relatively low cost, avoiding complicated processes, and special instruments. In the past decades, most of the research on liquid-phase synthesis of anisotropic nanocrystals have largely focused on II–IV semiconductor systems,^{14–20} but other systems reported in the literature are very limited. Recently, copper-based nanowires and nanobelts have received increasing attention because of their potential application in optoelectronic devices, catalysis, and superconductors. Orthorhombic Cu(OH)₂ is a well-known layered material. The magnetic properties of Cu(OH)₂ are remarkably sensitive to the intercalation of molecular anions,^{21–23} making the material a candidate for sensor applications. Cu(OH)₂ nanowires have been thought to be the precursors for the synthesis Cu₂O nanowires.²⁴ Up to now, the literature reported about synthesis of Cu(OH)₂ nanowires through a solution-phase approach is extremely sparse. Only in recent studies, Yang et al. reported that Cu(OH)₂ nanoribbons with a high aspect ratio were prepared by coordination self-assembly in solution using Cu₂S nanowires as precursors,²⁵ and Cu(OH)₂ and CuO nanoribbon were also successfully synthesized on a copper surface in a controlled fashion.²⁶ Here, a new strategy is applied. We have made use of two immiscible liquids such as *n*-heptane and water, with metal precursor (Cu(DEHP)₂ in organic layer and NaOH in aqueous layer. The synthesis of the Cu(OH)₂ nanowires is accomplished at static aqueous–organic interface under ambient condition.

CuO nanowires and nanorods are also obtained at mild condition. Cupric oxide has been extensively studied because of its close connection to high *T_c* superconductors.^{27–29} CuO has also been known as a p-type semiconductor that exhibits a narrow band gap (1.2 eV) and has been widely exploited for

use as a powerful heterogeneous catalyst to convert hydrocarbons completely into carbon dioxide and water.³⁰ Moreover, it was reported by several groups that CuO could exist in as many as three different magnetic phases.^{31–33} So far, CuO nanowires have been mostly prepared by high-temperature approaches.^{34–36} In this report, CuO nanowires and nanorods are synthesized by dehydration of Cu(OH)₂ under ambient conditions at high concentrations of NaOH.

Experimental Section

Preparation. Bis(ethylhexyl) hydrogen phosphate (HDEHP) was purified by copper salt crystallization.³⁷ Other agents used in this work were analytic grades. Cu(DEHP)₂ was prepared by the following procedure:³⁸ HDEHP and the CuCl₂ in a 2:1 molar ratio was dissolved in heptane and water, respectively. CuCl₂ aqueous solution was mixed with the proper quantity of HDEHP solution, the aqueous phase was adjusted to pH = 6 by adding NaOH solution, and the organic phase was separated, washed with water five times, and then dried in a vacuum.

A typical synthesis of a Cu(OH)₂ nanowire was carried out as follows. A 0.05 M solution (20 mL) of Cu(DEHP)₂ in *n*-heptane was injected into 20 mL of 0.05 M NaOH aqueous solutions using a syringe with minimal disturbance in a 50-mL test tube at room temperature. After several minutes, a blue precipitate gradually grew at the interface. The reaction was accomplished at the static organic/aqueous biphasic boundary. Finally, the samples were taken out of the reactor after a given reaction time, washed with absolute alcohol and deionized water three times, and dried in air.

Characterization. X-ray powdered diffraction (XRD) measurements of the as-prepared sample were carried on a Japan Rigaku D/max-γA 200 X-ray diffractometer with Cu Kα radiation (λ = 1.54178 Å). Transmission electron microscopy (TEM) images were taken on a JEM-100CXII transmitting electric microscope (made in Japan), operating at 80 kV voltage. TEM analysis was prepared by placing of drop of colloidal solution onto the Formvar-covered copper grid. High-resolution TEM (HRTEM) images were obtained on Technai F30 at 300 kV.

Results and Discussion

Figure 1 shows the XRD pattern of a prepared sample. All the peaks can be indexed to orthorhombic Cu(OH)₂, in good

* To whom all correspondences should be addressed. E-mail: songxy@sdu.edu.cn.

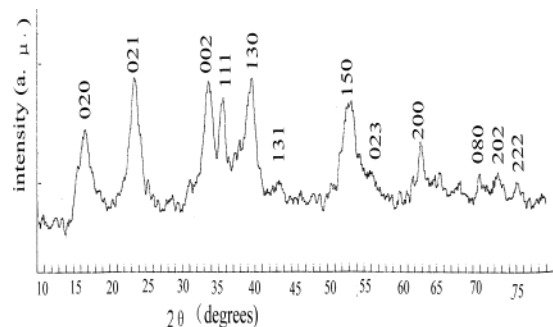


Figure 1. XRD pattern of the $\text{Cu}(\text{OH})_2$ of a sample prepared at the static interface.

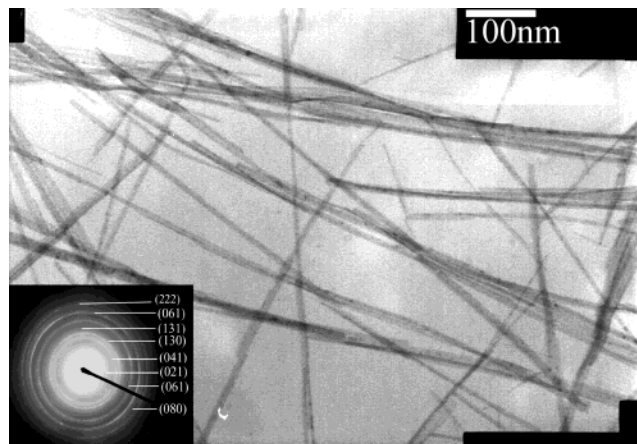


Figure 2. TEM image of $\text{Cu}(\text{OH})_2$ prepared at $\text{Cu}(\text{DEHP})_2 = 0.05 \text{ M}$ in *n*-heptane and $\text{NaOH} = 0.05 \text{ M}$ after aging 2 h.

agreement with JCPDS(13-0420). A conspicuous feature of the $\text{Cu}(\text{OH})_2$ crystals is their broadness, which indicates the small size of the $\text{Cu}(\text{OH})_2$ crystals.²⁵ A typical TEM image of the sample is given in Figure 2. As can be seen, all samples dispersed on the TEM grids display wirelike morphology with lengths of up to $3\text{--}4 \mu\text{m}$. It appears that the sample in Figure 2 consist of the single nanowire with the typical width of $4\text{--}5 \text{ nm}$ and the bundled nanowires with diameters of $8\text{--}10 \text{ nm}$. In comparison to the single nanowire, the bundled nanowires usually consist of $2\text{--}4$ single nanowires. It is clearly seen that the $\text{Cu}(\text{OH})_2$ nanowires are relatively straight and long, resulting in a large aspect ratio. The inset of Figure 2 shows a select area electron diffraction (SAED) pattern taken from the region including lots of nanowires, in which the primary ring pattern, diffraction induced by polycrystal, can be indexed with the orthorhombic $\text{Cu}(\text{OH})_2$.

High-resolution TEM (HRTEM) images of the single and a bundled $\text{Cu}(\text{OH})_2$ nanowire are shown in Figure 3, respectively. Evidently, both types of $\text{Cu}(\text{OH})_2$ nanowires are polycrystalline rather than a single crystal, and there is no specific orientational relationship among the grains. The result in our case is analogous to the $\text{Cu}(\text{OH})_2$ nanowires synthesized by Wang Zhonglin.³⁹

To understand the growth process of $\text{Cu}(\text{OH})_2$ nanowires, we have studied the effect of the reaction time. Parts a–c of figure 4 show TEM images of the sample grown at room temperature for 10 min, 30 min, and 3 h, respectively. As shown in Figure 3a, after 10 min, short wirelike crystals with lengths of $200\text{--}300 \text{ nm}$ and diameters of several nanometers were observed. With the increase of the reaction time, the nanowires became longer. For a reaction time up to 3 h, $\text{Cu}(\text{OH})_2$ nanowires grew much longer ($4\text{--}5 \mu\text{m}$ long).

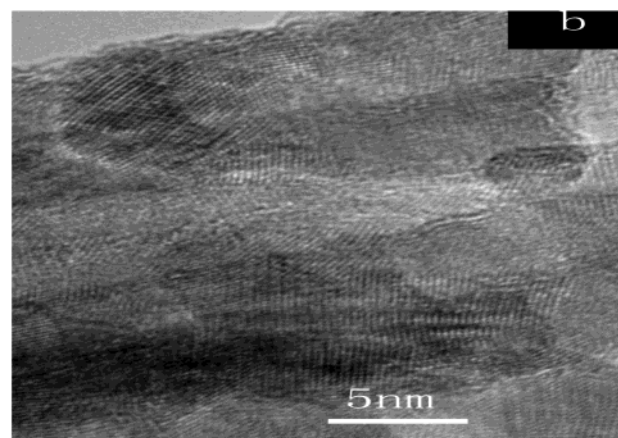
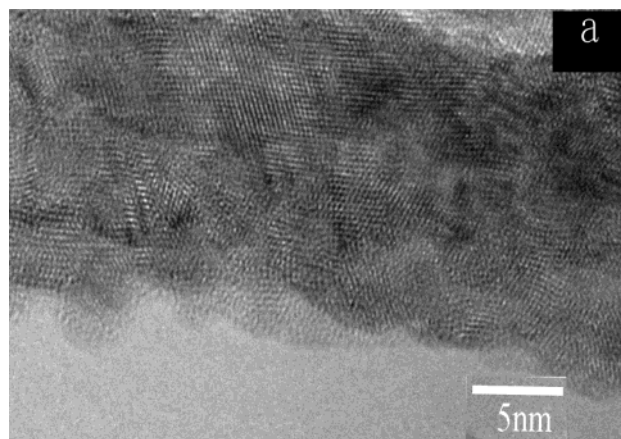


Figure 3. (a) HRTEM images of a single nanowire of $\text{Cu}(\text{OH})_2$. (b) HRTEM images of a bundle of nanowires.

However, if the organic phase containing $\text{Cu}(\text{DEHP})_2$ complexes was added into the aqueous phase containing NaOH under violent stirring, or the biphasic mixture composed of organic phase and aqueous phase was shaken for 30 min at the beginning of the reaction under the same condition, only short $\text{Cu}(\text{OH})_2$ rods were obtained (see Figure 5). Even after growth for 24 h, the nanowires were still only ca. 200 nm long. Furthermore, it can be seen from Figure 5 that many $\text{Cu}(\text{OH})_2$ whiskers lined up in parallel and formed bundlelike structures.

The exact mechanism for the formation of the $\text{Cu}(\text{OH})_2$ nanowires was still under investigation. The product formed at the interface showed wirelike morphology on the basis of the design strategy and the experiment results; a mechanism was put forward to explain the formation of the $\text{Cu}(\text{OH})_2$ nanowires. As is well known, Cu^{2+} prefers square planar coordination by OH^- , which led to form an olated chain. These olated chains can be connected through the coordination of OH^- to d_z^2 of Cu^{2+} , forming a two-dimensional (2D) structure. Finally, the 2D layers are stacked through the relatively weak coupling interactions, and become a three-dimensional (3D) crystal.²⁵ However, a key point is that, in a complex and highly nonequilibrium reaction system, the crystal growth rate is expected to be quite different, which determines the ultimate morphology of the products. For the $\text{Cu}(\text{DEHP})_2$ complex considered in our experiment, it has a square-planar symmetry.³⁸ After the $\text{Cu}(\text{DEHP})_2/n$ -heptane solution was injected into the NaOH aqueous solution, the formed solution exhibited a two-phase state. At the organic–aqueous phase interface, the hydrophobic hydrocarbon chains of $\text{Cu}(\text{DEHP})_2$ tended to extend into the organic phase, while the polar groups ($-\text{PO}_4$ parts) of $\text{Cu}(\text{DEHP})_2$ tended to extend into the aqueous solution.

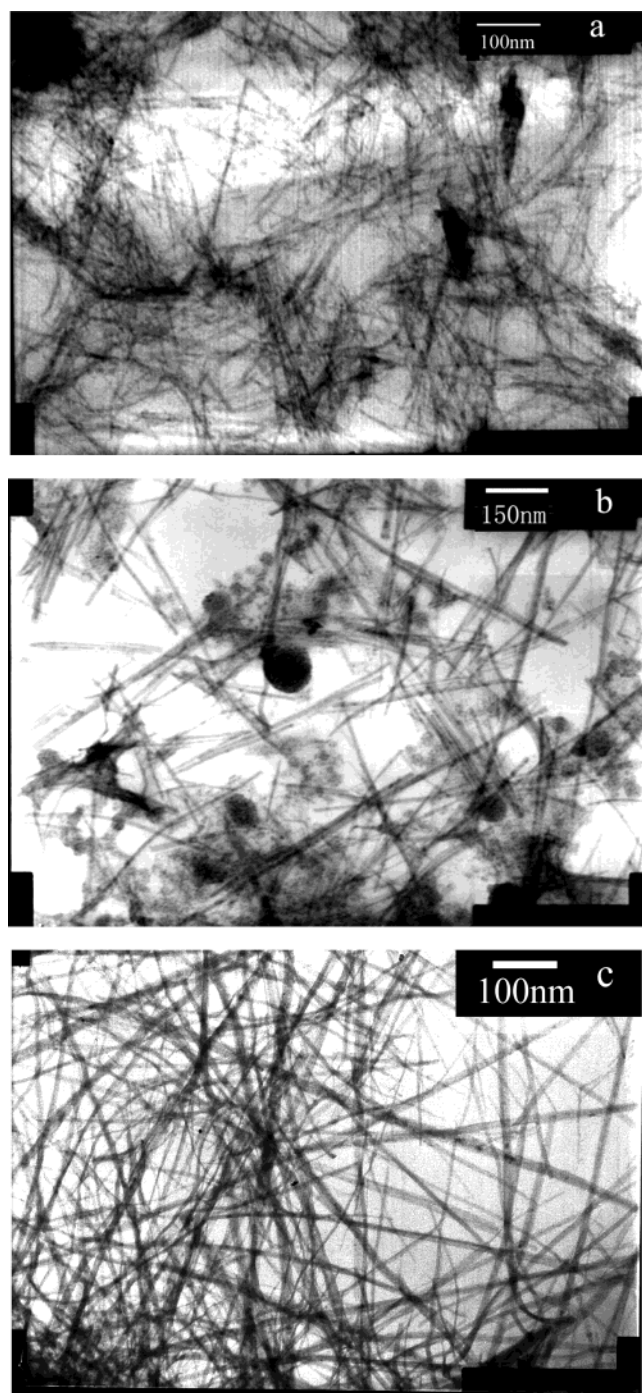


Figure 4. TEM images of $\text{Cu}(\text{OH})_2$ nanowires synthesized at different durations at $\text{Cu}(\text{DEHP})_2 = 0.05 \text{ M}$ in *n*-heptane and $\text{Na}(\text{OH})_2 = 0.05 \text{ M}$. (a) 10 min (b) 30 min (c) 3 h.

Therefore, from the structural character of $\text{Cu}(\text{DEHP})_2$, it can be predicted that the most energetically favorable existing form for this Cu complex at the interface should be that the plane involving Cu and its four coordination $-\text{O}$ atoms is perpendicular to the organic–aqueous interface (see Figure 6). Because of the large steric inhibition from the plane of complex, the OH^- groups diffusing at the interface preferentially attacked the complex along the two opposite directions out of $\text{Cu}(\text{O}-)_4$ plane. The deriving force was the competitive ability of coordinating to Cu^{2+} center between OH^- and PO^- groups. Because the two $\text{P}-\text{O}$ bonds actually were basically averaged and were between the normal $\text{P}-\text{O}^-$ single bond and the $\text{P}=\text{O}$ double bond in the $\text{Cu}(\text{DEHP})_2$ complex, their Lewis basicity

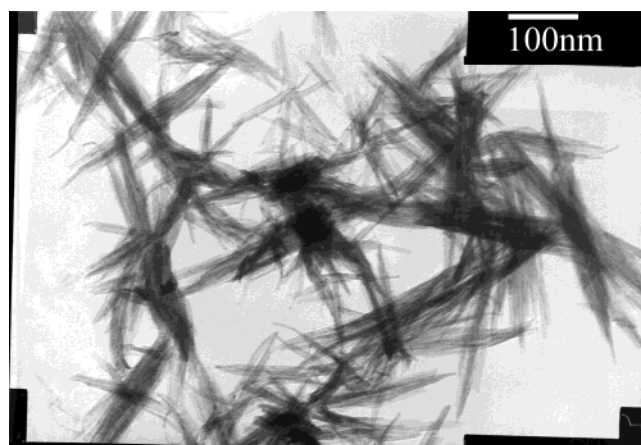


Figure 5. TEM of the $\text{Cu}(\text{OH})_2$ products obtained by shaking the biphasic mixture composed of $\text{Cu}(\text{DEHP})_2 = 0.05 \text{ M}$ in *n*-heptane and $\text{NaOH} = 0.05 \text{ M}$ in aqueous phase.

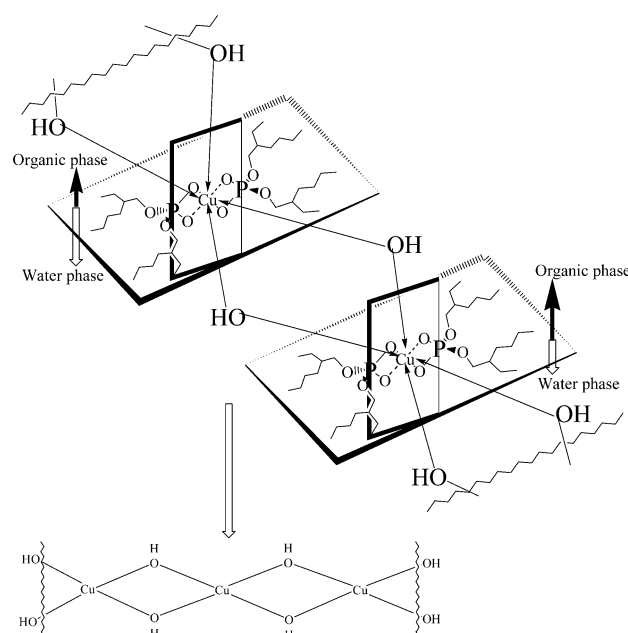


Figure 6. Schematic illustration for the formation process of the $\text{Cu}(\text{OH})_2$ nanowires.

was obviously smaller than that of OH^- , and the coordination interaction between Cu^{2+} and OH^- should be greater than that between Cu^{2+} and $\text{P}-\text{O}^-$. During the interaction process of the OH^- anions with the copper ions in the complex, the bonds between Cu^{2+} and the two $\text{O}(-\text{P})$ coordination atoms of DEHP became weaker, and the bonds between Cu^{2+} and O^{2-} (OH^-) were formed little by little, as the interaction between Cu^{2+} and OH^- groups increased. Once a $\text{Cu}(\text{OH})_4^{2-}$ core was formed, the quasi-1D $\text{Cu}(\text{OH})_2$ nanowires were formed by using two OH^- groups to bridge two Cu^{2+} centers in each $[\text{Cu}^{2+}-(\mu-\text{OH})_2-\text{Cu}^{2+}]$ unit. The procedure can be thought as a self-assembly one of the product morphology, as the scheme shown in Figure 6. Apparently, in the growth process of $\text{Cu}(\text{OH})_2$ nanowires, the ligand DEHP took as a template controller, which could effectively control the steric reorientation of $\text{Cu}(\text{DEHP})_2$ and limit the OH^- attack direction. Furthermore, it was noted that the ordered arrangement of $\text{Cu}(\text{DEHP})_2$ molecules at the interface also provided a favorable condition for the growth of $\text{Cu}(\text{OH})_2$ nanowires. This growth mechanism of $\text{Cu}(\text{OH})_2$ nanowires from a complex with large steric inhibition might be similar to those reported in refs 40 and 41.

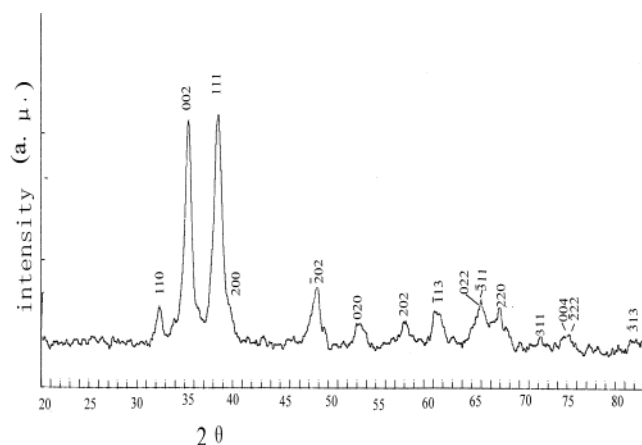


Figure 7. XRD pattern of CuO obtained through dehydration of $\text{Cu}(\text{OH})_2$ at $\text{Cu}(\text{DEHP})_2 = 0.05$ M and $\text{NaOH} = 0.1$ M.

However, under violent stirring, the well-ordered arrangement of the $\text{Cu}(\text{DEHP})_2$ molecules at the static interface was destroyed, and the systematic order was reduced to small area. Under disordered reaction conditions, the bridging effect of OH^- anions was too limited to connect copper cations of every unit to form enough long chains. As a result, only short $\text{Cu}(\text{OH})_2$ whiskers were obtained. It was further confirmed that the ordered arrangement of the complexes at the interface was crucial to the growth of $\text{Cu}(\text{OH})_2$ nanowires. Moreover, under stirring or shaking, every $\text{Cu}(\text{DEHP})_2$ molecule of the organic media has a chance to contact with OH^- ions. Therefore, the amount of nucleation sites of $\text{Cu}(\text{OH})_2$ generated at the same time in the mixed solution was much higher than that formed at the static interface between the organic phase and the aqueous phase. As a result, more $\text{Cu}(\text{OH})_2$ grew at the same, and they can easily bundle together to form a relatively aligned structure.

We also discovered that the concentration of NaOH played an important factor for the growth of the $\text{Cu}(\text{OH})_2$ nanowires. Keeping other conditions same, several comparative experiments were made in the range from 0.05 to 0.2 M of the concentration of NaOH. When the concentration of NaOH in aqueous phase was less than 0.1 M, the blue products formed at the interface could stably exist after a given aging time. While at $\text{NaOH} = 0.1$ M, after reacting for 2–3 h, the initial blue precipitation produced at the interface gradually turned into black products under ambient temperature. After a given reaction time, the blue precipitation was completely transformed into black products. XRD pattern of the black sample is shown as the spectrum in Figure 7. All the diffraction peaks of Figure 7 can be indexed to monoclinic CuO (JCPDS(41-254)). Figure 8a presents a low magnification TEM image of the CuO sample. Apparently, the CuO nanowires are also obtained. As is shown in Figure 8a, the wirelike morphology is well preserved after dehydration of $\text{Cu}(\text{OH})_2$ nanowires; only a part of the product displays beltlike structure with about 50–80 nm in width. A higher magnification TEM image in Figure 8b shows that wirelike $\text{Cu}(\text{OH})_2$ is either a single nanowire or a bundle of the nanowires. The bundled nanowires usually array with several single nanowires. By increasing the concentration of NaOH, the transformation rate from $\text{Cu}(\text{OH})_2$ to CuO becomes much faster. At the $\text{NaOH} = 0.2$ M, after injecting the $\text{Cu}(\text{DEHP})_2$ *n*-heptane into the jar containing NaOH aqueous solution for 20 min, the blue products first generated at the interface started to transform into black products. TEM in Figure 8c showed that only short CuO whiskers were obtained. In general, the orthorhombic $\text{Cu}(\text{OH})_2$ is unstable oxolation because oxygen atoms are either pentacoordinated or tricoordinated. It can be easily transformed to monoclinic CuO

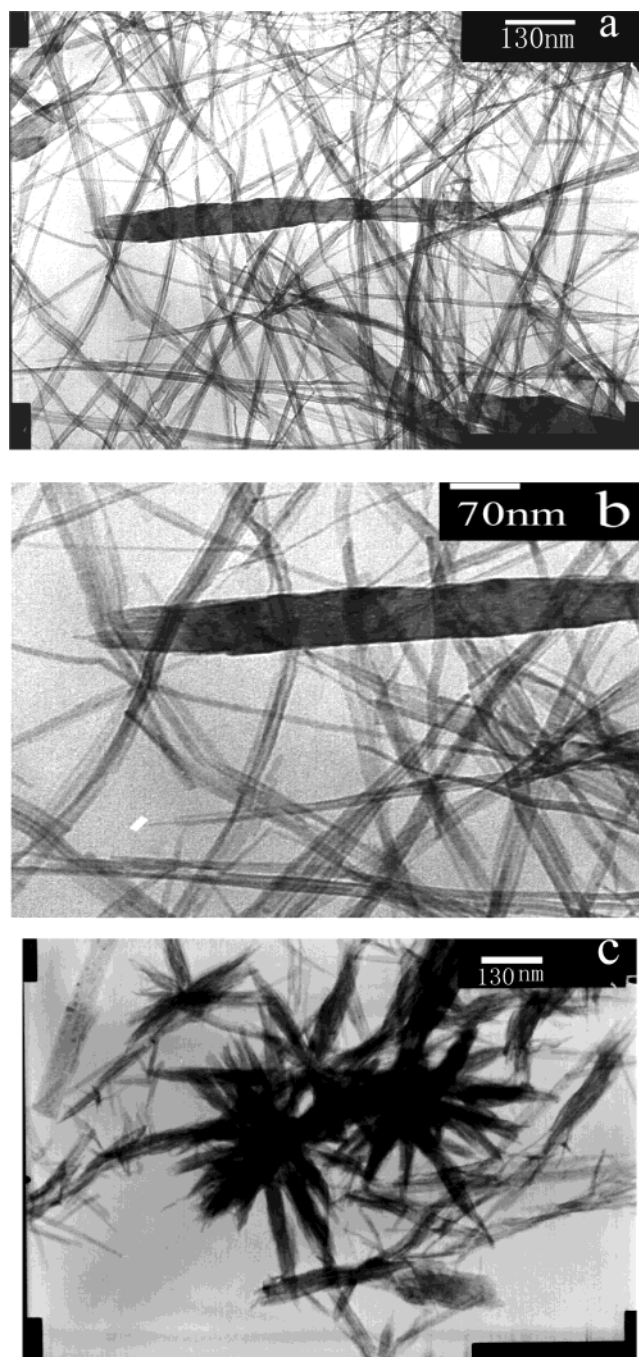


Figure 8. TEM images of CuO obtained from the dehydration of $\text{Cu}(\text{OH})_2$ at the different concentrations of NaOH (a) and (b) $\text{Cu}(\text{DEHP})_2 = 0.05$ M and $\text{NaOH} = 0.1$ M at different magnifications. (c) $\text{Cu}(\text{DEHP})_2 = 0.05$ M and $\text{NaOH} = 0.2$ M.

under certain reaction conditions such as high pH or through heat treatment.⁴² Under the highly basic condition, the free OH^- in solution may act as a nucleophile to the H^+ located at the bridging $>\text{O}$ centers, forming H_2O molecules with a H bond back to the bridging $>\text{O}^{2-}$ centers. On the other hand, from the viewpoint of the ion polarization, since Cu^{2+} has a stronger polarizing ability to other anions compared with the alkaline cations, the deformation of the electron cloud of the bridging $>\text{O}^{2-}$ ion is larger. As a result, the electron transfer from the bridging $>\text{O}^{2-}$ to Cu^{2+} is more, the acidity of the linked proton H^+ is larger, and the proton release is more likely. Therefore, in the more basic medium, the excess free OH^- anions in solution may easily capture these more acidic H^+ s, forming the $>\text{O}\cdots\text{HOH}$ moieties via a proton transfer from the bridging

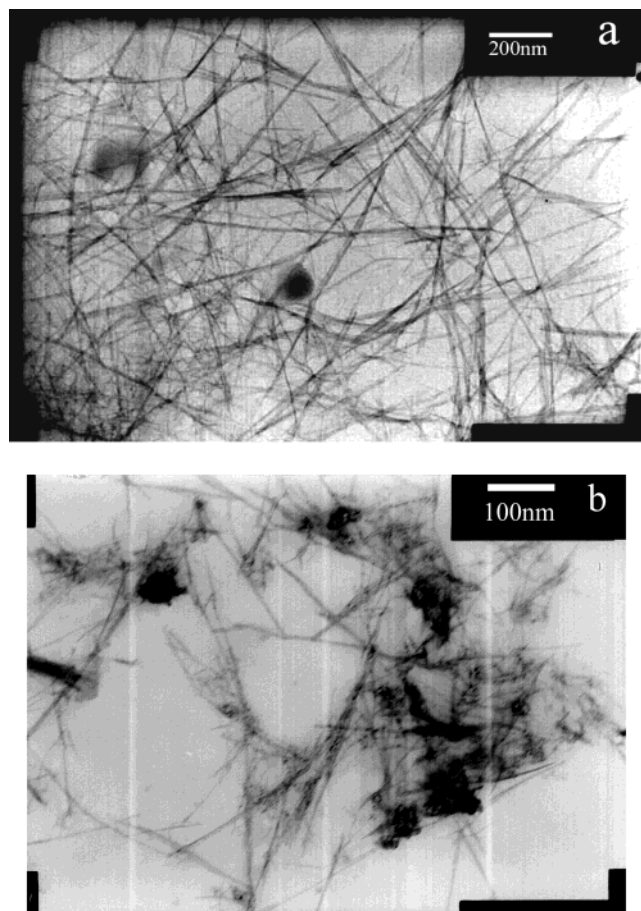


Figure 9. TEM images of the Cu(OH)_2 obtained at the static interface between (a) $\text{Cu(DEHP)}_2 = 0.05 \text{ M}$ in *n*-hexene and $\text{NaOH} = 0.05 \text{ M}$ and (b) $\text{Cu(DEHP)}_2 = 0.05 \text{ M}$ in CHCl_3 and $\text{NaOH} = 0.05 \text{ M}$.

$>\text{OH}$ to OH^- . These formed H_2O molecules more easily depart away because the coupling interaction between the formed H_2O and the remainder bridging $>\text{O}$ centers is weak. Obviously, the more basic the medium, the greater the free OH^- concentration, the more the possibility of OH^- to capture the H^+ linked to the bridging $>\text{O}$ centers per unit time. Therefore, with an increase of the NaOH concentration, the transformation rate of the Cu(OH)_2 products to monoclinic CuO becomes faster. In this experiment, under the condition of the relatively low concentration of $\text{NaOH} = 0.1 \text{ M}$, Cu(OH)_2 products could spontaneously turn to CuO at ambient temperature. This phenomenon might be related to the small sizes of Cu(OH)_2 formed at the static interface. On the other hand, by using the organic phase as a buffer to separate Cu^{2+} and OH^- , the explosive reaction can be made less vigorous, which can facilitate to form Cu(OH)_2 having a flexible and loose structure. The Cu(OH)_2 products with loose structure might transform more easily into CuO in comparison with those large bulk products.

For comparison, we selected other organic solvents in which to dissolve Cu(DEHP)_2 . By replacing *n*-heptane with *n*-hexane, *n*-hexene, and *n*-octane at the same experiment condition, respectively, long Cu(OH)_2 nanowires were also obtained (See Figure 9a). However, in chloroform solvent, only short Cu(OH)_2 wiskers with length of ca. 200–300 nm were observed (see Figure 9b). These differences indicated that the organic solvent properties also affected the sizes and morphology of Cu(OH)_2 . For this experimental phenomenon, it might be explained as follows. There were different solute–solvent interactions in both cases. As is known, those nonpolar solvents such as *n*-heptane did not possess any active functional groups, the interaction in

Cu(DEHP)_2 /*n*-heptane solution was the van der Waals interaction forces between *n*-heptane solvent molecules and the alkyl group chains. However, in Cu(DEHP)_2 /chloroform solutions, there were not only the van der Waals interaction forces between the alkyl group chains and the chloroform molecules, but also the slightly weak hydrogen-bonding interaction between $\text{H}-\text{CCl}_3$ and the polar groups ($\text{P}-\text{O}$).⁴⁰ Obviously, this additional hydrogen bonding might weaken the coupling interaction between the Cu center and coordination O atoms, resulting in the release rate of Cu^{2+} ions faster. In this case, the nucleation rate of Cu(OH)_2 at the interface between the polar solvent/aqueous phase was relatively faster in comparison to those between the nonpolar solvent/aqueous. We assumed that it was helpful for the formation of Cu(OH)_2 nanowires when the rate of connection of copper ions and OH^- matched the rate at which DEHP^- was lost. When the loss of DEHP^- was faster, it was not favorable for the formation of Cu(OH)_2 nanowires; only short Cu(OH)_2 wiskers were obtained. From the above analysis, it can be known that solvent polarity may affect the coordination strength of DEHP^- to Cu^{2+} , which can further affect the morphology of the products.⁴⁴ Therefore, the choice of solvent played a key role in synthesizing of Cu(OH)_2 nanowires.

Conclusion

In summary, we have successfully synthesized Cu(OH)_2 nanowires at the liquid–liquid interface by taking a metallo-organic precursor in the organic layer and the appropriate alkaline concentrations in the aqueous layer. These nanowires are several nanometers in width, and up to 4 μm in length. From the above study, it can be known that the novel structure of the Cu(DEHP)_2 and its orderly arrangement at the interface played a significant role in the formation of Cu(OH)_2 nanowires. Furthermore, we have also demonstrated that wirelike and wiskerlike CuO products can conveniently be obtained by dehydration of Cu(OH)_2 under ambient condition. It is well known that HDEHP as an extractant can interact with many metal ions of the aqueous phase to form complexes (M(DEHP)_2). We hope this method can extend to fabricate similar inorganic materials.

Acknowledgment. This work was supported by the National Science Foundation of China (NSFC 20171029).

References and Notes

- (1) Hu, J. T.; Odom, T. W.; Lieber, C. M. *Acc. Chem. Res.* **1999**, *32*, 435.
- (2) Ozin, G. A. *Adv. Mater.* **1992**, *4*, 612.
- (3) Wu, Y. Y.; Yang, P. D. *Chem. Mater.* **2000**, *12*, 605.
- (4) Liang, C. H.; Meng, G. W.; Lei, Y.; Philipp, F.; Zhang, L. D. *Adv. Mater.* **2001**, *13*, 1330.
- (5) Morales, A. M.; Lieber, C. M. *Science* **1998**, *279*, 208.
- (6) Zhang, Y. F.; Tang, Y. H.; Wang, N.; Yu, D. P.; Lee, C. S.; Bello, L. S. *Appl. Phys. Lett.* **1998**, *72*, 1835.
- (7) Yazawa, M.; Koguchi, M.; Muto, A.; Hiruma, K. *Appl. Phys. Lett.* **1992**, *61*, 2051.
- (8) Choi, Y. C.; Kim, W. S.; Park, Y. S.; Lee, S. M.; Bae, D. J.; Lee, Y. H.; Park, G. S.; Choi, W. B.; Lee, N. S.; Kim, J. M. *Adv. Mater.* **2000**, *12*, 746.
- (9) Huang, M. H.; Choudrey, A.; Yang, P. *Chem. Commun.* **2000**, *12*, 1063.
- (10) Zhang, J. H.; Yang, X. G.; Wang, D. W.; Li, S. D.; Xie, Y.; Xia, Y. N.; Qian, Y. T. *Adv. Mater.* **2000**, *12*, 1348.
- (11) Qi, L. M.; Ma, J. M.; Cheng, H. M.; Zhao, Z. G. *J. Phys. Chem. B* **1997**, *101*, 3460.
- (12) Murphy, C. J.; Jana, N. R. *Adv. Mater.* **2002**, *14*, 80.
- (13) Rees, G. D.; Gowing, R. E.; Hammond, S. J.; Robinson, B. H. *Langmuir* **1999**, *15*, 1993.
- (14) Li, Y. D.; Liao, H. W.; Ding, Y.; Qian, Y. T.; Li, Y.; Zhou, G. E. *Chem. Mater.* **1998**, *10*, 2301.
- (15) Wang, W. Z.; Geng, Y.; Yan, P.; Liu, F. Y.; Xie, Y.; Qian, Y. T. *Inorg. Chem. Commun.* **1999**, *2*, 83.

- (16) Yan, P.; Xie, Y.; Qian, Y. T.; Liu, X. M. *Chem. Commun.* **1999**, 1293.
- (17) Deng, Z. X.; Wang, C.; Sun, X. M.; Li, Y. D. *Inorg. Chem.* **2002**, *41*, 869.
- (18) Manna, L.; Scher, E. C.; Alivisatos, A. P. *J. Am. Chem. Soc.* **2000**, *122*, 12700.
- (19) Qing, Y.; Tang, K. B.; Wang, Ch. R.; Qian, Y. T.; Zhang, Sh. Y. *J. Phys. Chem. B* **2002**, *106*, 9227.
- (20) Chen, C. C.; Chao, C. Y.; Lang, Z. H. *Chem. Mater.* **2000**, *12*, 1516.
- (21) Fujita, W.; Awaga, K. *Synth. Met.* **2001**, *122*, 569.
- (22) Fujita, W.; Awaga, K. *Inorg. Chem.* **1996**, *35*, 1915.
- (23) Fujita, W.; Awaga, K. *J. Am. Chem. Soc.* **1997**, *119*, 4563.
- (24) Wang, W. Z.; Wang, G. H.; Wang, X. S.; Zhang, R. J.; Liu, Y. K.; Zheng, C. L. *Adv. Mater.* **2002**, *14*, 67.
- (25) Wen, X. G.; Zhang, W. X.; Yang, S. H.; Dai, Z. R.; Wang, Z. L. *Nano Lett.* **2002**, *2*, 1397.
- (26) Wen, X. G.; Zhang, W. X.; Yang, S. H. *Langmuir* **2003**, *19*, 5898.
- (27) Wu, M. K.; Ashburn, J. R.; Torng, C. J.; Hor, P. H.; Meng, R. L.; Gao, L.; Huang, Z. J.; Wang, Y. Q.; Chu, C. W. *Phys. Rev. Lett.* **1987**, *58*, 908.
- (28) Schon, J. H.; Dorget, M.; Beuran, F. C.; Zu, X. Z.; Arushanov, E.; Cavellin, C. D.; Laugues, M. *Nature* **2001**, *414*, 434.
- (29) Hodges, J. A.; Sidis, Y.; Bourges, P.; Mirebeau, I.; Hennion, M.; Chaud, X. *Phys. Rev. B* **2002**, *66*, 020501.
- (30) Reitz, J. B.; Solomon, E. *J. Am. Chem. Soc.* **1998**, *120*, 11467.
- (31) Forsyth, J. B.; Brown, P. J.; Wanklyn, B. M. *J. Phys. C: Solid State Phys.* **1988**, *21*, 2917.
- (32) Yang, B. X.; Thurston, T. R.; Tranquada, J. M.; Shirane, G. *Phys. Rev. B* **1989**, *39*, 4343.
- (33) Sukhorukov, Y. P.; Loshkareva, N. N.; Samokhvalov, A. A.; Naumov, S. V.; Moskvina, A. S.; Ovchinnikov, A. S. *J. Magn. Magn. Mater.* **1998**, *183*, 356.
- (34) Suzuki, H.; Hukuzawa, N.; Tanigaki, T.; Sato, T.; Kido, O.; Kimura, Y.; Kaito, C. *J. Cryst. Growth* **2002**, *244*, 168.
- (35) Jiang, X. C.; Herricks, T.; Xia, Y. N. *Nano Lett.* **2002**, *2*, 1333.
- (36) Wang, S. H.; Huang, Q. J.; Wen, X. G.; Li, X. Y.; Yang, S. H. *Phys. Chem. Chem. Phys.* **2002**, *4*, 3425.
- (37) Long, H. Y.; Lu, H. Y. *At. Energy Sci. Technol.* **1964**, *6*, 742.
- (38) Yu, Z. J.; Ibrahim, T. H.; Neuman, R. D. *Solvent Extr. Ion Exch.* **1998**, *16* (6), 1437.
- (39) Wang, Z. L.; Kong, X. Y. *J. Phys. Chem. B* **2003**, *107*, 8275.
- (40) Li, Y. D.; Sui, M.; Ding, Y.; Zhang, G. H.; Zhuang, J.; Wang, C. *Adv. Mater.* **2000**, *12*, 818.
- (41) Xiong, Y. J.; Xie, Y.; Du, G. D.; Liu, X. M.; Tian, X. B. *Chem. Lett.* **2002**, 98.
- (42) Zhang, W. X.; Wen, X. G.; Yang, S. H. *Inorg. Chem.* **2003**, *16*, 5005.
- (43) Li, L. M.; Xu, G. X. *Acta Chim.* **1984**, *1*, 1.
- (44) Chen, M.; Xie, Y.; Lu, J.; Xiang, X. J.; Zhang, S. Y.; Qian, Y. T.; Liu, X. M. *J. Mater. Chem.* **2002**, *12*, 748.